Research Article | Vol. 30, No. 12 / 6 Jun 2022 / Optics Express 21535

Optics EXPRESS

Direct generation of high brightness path entangled N00N states using structured crystals and shaped pump beams

GIUSEPPE DI DOMENICO,[1,*] SHAUL PEARL,[1,2] AVIV KARNIELI,[1] SIVAN TRAJTENBERG-MILLS,[1] IRIT JUWILER,[3] HAGAI S. EISENBERG,[4] AND ADY ARIE[1]

[1]School of Electrical Engineering, Fleischman Faculty of Engineering, Tel-Aviv University TAU, Tel-Aviv 69978, Israel
[2]Applied Physics Department, Soreq NRC, Yavne 81800, Israel
[3]Department of Electrical and Electronics Engineering, Sami Shamoon College of Engineering, Ashdod 77245, Israel
[4]Racah Institute of Physics, Hebrew University of Jerusalem, Jerusalem 91904, Israel
[*]giuseppedidomenico8@gmail.com

Abstract: Optical N00N states are N-photon path entangled states with important applications in quantum metrology. However, their use was limited till now owing to the difficulties of generating them in an efficient and robust manner. Here we propose and experimentally demonstrate two new simple, compact and robust schemes to generate path entangled N00N states with $N = 2$ that emerge directly from the nonlinear interaction. The first scheme is based on shaping the pump beam, and the second scheme is based on modulating the nonlinear coefficient of the crystal. These new methods exhibit high coincidence count rates for the detection of a N00N state, reaching record value of 2×10^5 coincidences per second. We observe super-resolution by measuring the second order correlation on the generated N = 2 state in an interferometric setup, showing the distinct fringe periodicity at half of the optical wavelength. Our findings may pave the way towards scalable and efficient sources for super-resolved quantum metrology applications and for the generation of bright squeezed vacuum states.

1. Introduction

Efficient and reliable sources of entangled states are crucial in quantum information technologies [1]. Examples include studies of nonlocality [2], quantum computation [3,4], simulation [5,6], communication [7], and quantum metrology [8–12]. The realization of many of these applications requires the generation of N00N states [13–16], which are entangled states with N particles of the form $|\psi\rangle = (|N\rangle|0\rangle + |0\rangle|N\rangle)/\sqrt{2}$. It is known [17] that in an interferometer, the N00N states improve the phase sensitivity by a factor of N compared to coherent states. Quantum metrology [18], super-resolved interferometry [19], lithography [20], quantum imaging [21] and quantum error correction [22] are all examples in which N00N states are beneficial due to the improved sensitivity. This super-resolution enables to improve the resolving power of interferometers beyond the standard quantum limit. Unfortunately, these states are not easily realized. Path entangled N00N states with $N = 2$ can be obtained via spontaneous parametric down conversion (SPDC) [23] process, where a pump photon splits into two identical daughter photons that propagate in two different modes, followed by a Hong-Ou-Mandel interference. The SPDC process itself is either non-collinear, and hence limited in efficiency, or collinear but requires additional components and degrees of freedom to separate the signal and the idler photons. The two identical photons must be carefully selected from the SPDC spectrum and then impinge simultaneously on a beam splitter; thus, it is necessary to ensure that the two paths

#451641 https://doi.org/10.1364/OE.451641
Journal © 2022 Received 20 Dec 2021; revised 25 Apr 2022; accepted 25 Apr 2022; published 1 Jun 2022

Optics EXPRESS

have exactly the same optical length. These schemes have been realized in free space [24–29] as well as in integrated photonics platforms [30,31] to generate path entanglement or polarization entanglement N00N states.

Here we propose two new ways to generate a path entangled N00N state with $N = 2$, i.e. $|\psi\rangle = (|2\rangle|0\rangle + |0\rangle|2\rangle)/\sqrt{2}$, in a compact, robust, and efficient manner either by shaping the pump beam; or by structuring the nonlinear coefficient of the crystal. The two experimental setups are presented in Fig. 1(a)) and (b)). Both methods enable the generation of these states directly from the nonlinear interaction without the need for any additional optical elements.

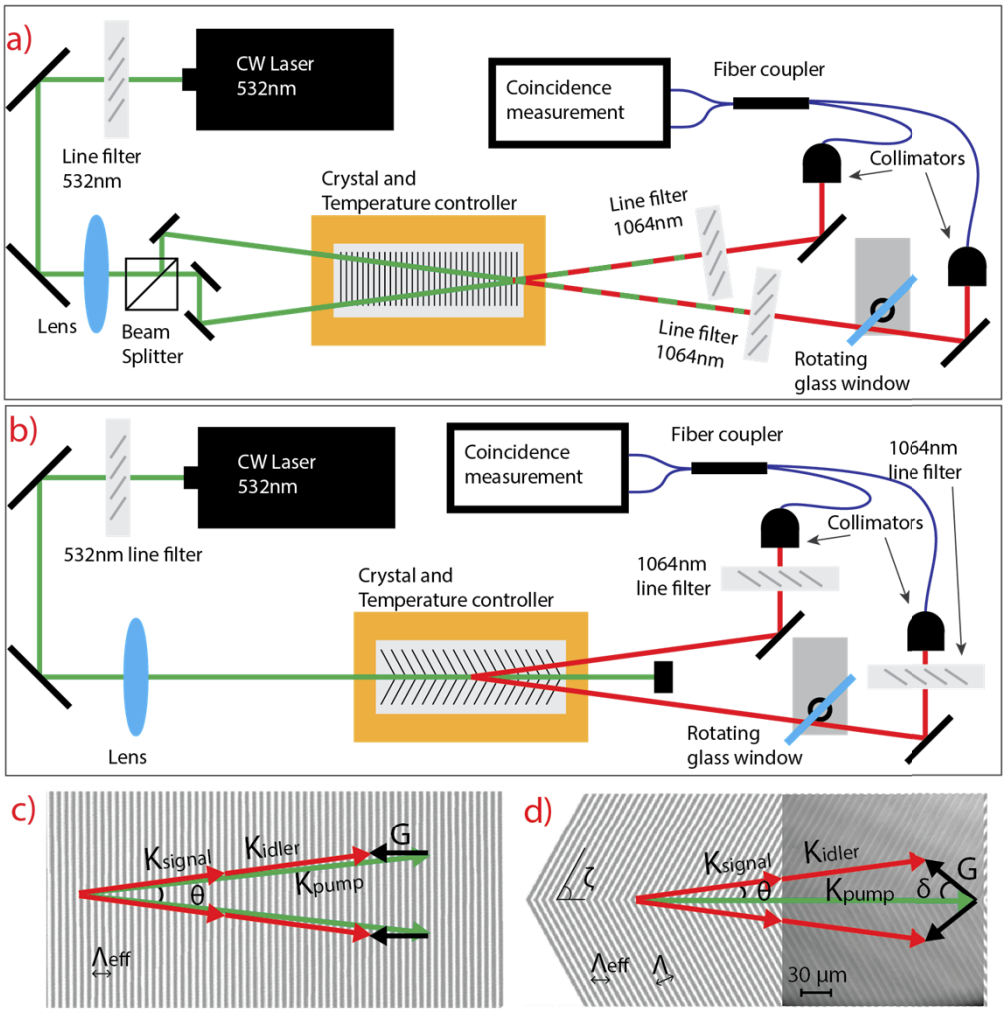

Fig. 1. Experimental setup for the characterization of the 2-photon N00N state (a) by pump shaping and (b) by a custom nonlinear V shaped crystal. (c) and (d) show the 2D poling design and the momentum conservation scheme of the SPDC processes relative to setups (a) and (b) respectively. The right part in (d) is a microscope image of the crystal top facet after selective etching.

The first approach is based on pump shaping. We illuminate the nonlinear crystal with two beams from the same laser source, as shown in Fig. 1(a)). In this case, the crystal itself is a standard periodically poled crystal, readily available in many current SPDC setups. This setup

Optics EXPRESS

has been previously investigated [24–27] to produce polarization-entangled states, rather than path entangled N00N states.

The second approach is based on crystal shaping. The use of shaped crystals, based on two-dimensional periodic modulation of the nonlinear coefficient for N00N state generation, has been previously investigated [28,29], but suffered from unwanted generation of photons from parasitic quasi phase matching (QPM) orders [28] and from relatively low generation rates [29]. Our new design is based on two tilted gratings forming a V shape, as shown in Fig. 1(d)). This design utilizes first order QPM with a one-dimensional poling pattern in each one of the chosen directions, therefore resulting with higher performance than the previous demonstrations.

The SPDC field emanating from the crystal facet splits into two well-defined modes, making them easy to collect. Further, due to the conservation of momentum, they are emitted in pairs, in either of the modes, which constitutes the desired N00N state. This unique property simultaneously overcomes the need to spatially filter the desired entangled pair from the rim of the phase-matching cone as well as the precise interference on a balanced beam-splitter, usually required for the N00N state generation. Thus, the process is highly efficient as well as uses a minimal number of optical components. To characterize the super-resolution properties of the N00N states in our setup, the pair production is followed by an interference stage. The signature of the generated N = 2 N00N state is an interference pattern with half the period relative to that of a classical state of light with the same wavelength.

We demonstrate our schemes with parametric down conversion from 532 nm to 1064 nm, but the same concept can be used at other wavelengths, by changing the poling periods in the periodically poled crystals. In both setups, a single longitudinal mode 532nm laser (ALPHALAS MONOPOWER-532-100-SM) with CW power up to 100mW and ~300m coherence length, was used as a pump source. A 532nm line filter with an extinction ratio of 70dB and transmission of ~60%, filtered the pump laser output to prevent seeding the SPDC by the residual 1064nm power of the laser. The laser beam was focused to a ~300μm spot diameter at the middle of the nonlinear crystal (NLC). In both setups, the two down-converted photons are emitted simultaneously and enter with equal probability into one of two possible pathways, where the difference between the two paths is kept below 1 mm. Thus, the photons form an entangled biphoton state

$$|\psi\rangle_{2002} = \frac{(|2\rangle|0\rangle + |0\rangle|2\rangle)}{\sqrt{2}} = \frac{((a^{\dagger})^2 + (b^{\dagger})^2)|0\rangle|0\rangle}{2}, \tag{1}$$

where $a^{\dagger}$ and $b^{\dagger}$ are the photon creation operators on the two paths.

For the pump beam shaping configuration, the focused 532nm beam is split into two equal beams using a beam splitter and three folding mirrors. The two beams are then directed into the NLC with ~1.6° angular separation inside the crystal, while maintaining the same optical length. The angular separation between the two beams allows us to easily swap from one setup to the other with minimal adjustment of the alignment. The NLC is a standard, 20 mm long PPKTP crystal with poling period of $\Lambda = 9\mu m$, anti-reflection coated for 1064/532 nm, kept at a temperature of 36 0.05°C. The equal pump splitting ensures that the two down-converted photons will have equal probabilities to be emitted into the two different directions, so the $|\psi\rangle_{2002}$ state of Eq. (1) is directly generated.

For the NLC shaping configuration, we use a 13mm-long periodically poled Mg-doped stoichiometric lithium tantalate (PPMgSLT) crystal kept at 31.5 0.05°C. The poling structure was a 2D V-shaped grating, which was fabricated by us using the electric-field poling method [32]. As described in the phase matching scheme in Fig. 1(d), the two adjacent regions of the structure phase match the emission of the down-converted photons in two separate directions. The effective periodicity of the V-shaped poling is $\Lambda_{eff} = \Lambda/cos\delta = 7.94\mu m$, where the opening half angle of the V structure is $\xi = 90^o - \delta = 66^o$. For this design the phase matching condition

Optics EXPRESS

requires:

$$\Lambda = \frac{2\pi sin\ \delta}{[(k_{siganl} + k_{idler})sin\ \theta]}, \tag{2}$$

$$\delta = \left[\frac{(k_{siganl} + k_{idler})sin\ \theta}{(k_{pump} - (k_{siganl} + k_{idler})cos\ \theta)}\right], \tag{3}$$

where $2\theta = 1.6^o$ is the separation angle that we chose between the two emission paths.

By pumping the NLC exactly along the boundary between the two regions, the down-converted photons have equal probability to be simultaneously emitted into one of the above possible directions, hence the process generates the desired N = 2 N00N state of Eq. (1). The equal probability results from the equal spatial overlap between the Gaussian pump beam and the two poled regions in the crystal. The advantage of this configuration relative to the previous one is that the pump beam travels on-axis, i.e. at a different direction with respect to the two paths of the down-converted photons, and as such it can be spatially filtered with high extinction. However, such a spatial beam splitting may cause diffraction loss and mode mismatch in the NLC that reduces the SPDC efficiency.

To demonstrate the super-resolution behavior of the generated N00N state, it was coupled into an interference setup. The creation operators, $a'^{\dagger}$ and $b'^{\dagger}$, after the unitary transformation by the phase-shifter and beam-splitter become [33]: $a'^{\dagger} = (e^{i\phi}a^{\dagger} + ib^{\dagger})/\sqrt{2}$ and $b'^{\dagger} = (ie^{i\phi}a^{\dagger} + b^{\dagger})/\sqrt{2}$. Hence, by substituting $a^{\dagger}$ and $b^{\dagger}$ in terms of $a'^{\dagger}$ and $b'^{\dagger}$, and using Eq. (1), the final state is:

$$\begin{aligned} |\psi\rangle_{2002} &= \frac{1}{4}[(e^{-i\phi}a'^{\dagger} - ie^{-i\phi}b'^{\dagger})^2 + (-ia'^{\dagger} + b'^{\dagger})^2]|0\rangle|0\rangle \\ &= \sin\phi\frac{|2\rangle|0\rangle + |0\rangle|2\rangle}{\sqrt{2}} + cos\phi|1\rangle|1\rangle. \end{aligned} \tag{4}$$

When a coincidence measurement is performed on the state of Eq. (4), only the $|1\rangle|1\rangle$ term is post-selected, which has an amplitude of $\cos(\phi)$ and hence probability of $\cos^2(\phi)$. The corresponding coincidence rate oscillates as $\cos^2(\phi)$, hence has a maximum every phase shift $\phi = q \cdot \pi$ (where q is an integer). This is the signature of super resolution, as the path difference between adjacent maxima oscillates at half the photon wavelength.

The down-converted photons in both configurations are filtered by either a 3 nm or 1 nm bandwidth line filter centered at 1064 nm and are then coupled to the two inputs of a single mode (SM) polarization-maintaining 50:50 fiber coupler/splitter. The down-converted photons' waist was matched to the SM fiber mode size for optimal coupling. The detection was performed using two superconducting nanowire single-photon detectors with an efficiency of 68% (Single Quantum Eos). The detectors are followed by an electronic time-tagging system (Swabian Time Tagger 20) to identify the time correlated single photon measurements. The tagging system counts coincidence events on the two different arms occurring within less than 1ns. The two arms have identical components and equal length. A rotating uncoated 0.19mm thick glass plate positioned at around 45° with respect to the optical axis is placed in one of the arms to control the relative phase between the two arms. Finally, the resulting change in the coincidence count rate is measured as a function of the phase shifter angle. The whole system is enclosed in a covered casing to avoid external disturbances.

The SPDC process of both the setups has been first studied with numerical simulations. Some approaches have been proposed to simulate the SPDC process [34–37]. The method we used in our study is based on solving the Heisenberg equations of motion for the electric field operators, that evolve under the SPDC Hamiltonian, and its details can be found in [36,37]. The simulations post-select one specific frequency from the emitted field, hence the process studied is strictly degenerate. Figures 2(a) and 2(b) show the results of the photo-detection probability in the far field of the crystal in the crossed-beam setup and the structured crystal case, respectively.

Optics EXPRESS

Two spots are clearly visible, confirming the advantages of our design, allowing for a selective, directed emission of photon pairs, with nearly no additional unwanted emissions. This in contrast to the conventional typical conical emission pattern of the SPDC signal. For the V-shaped configuration we experimentally verify that the emission directions are as predicted by the poling design. The inset in Fig. 2(b) shows an experimental 2D angular mapping of the pump and SPDC beams emerging from the NLC. This was done by raster scanning the output far-fields of the residual pump and the SPDC beams, using single mode optical fiber coupled to a single photon detector (Single Quantum). As can be seen, the two 1064nm beams deviate from the pump direction by ~ 0.8deg (the angles refer to propagation inside the crystal), as was designed and predicted by the simulation. Figures 2(c) and 2(d) are the simulated second order correlation measurements, $g^{(2)}$ over the x-axis for $y = 0$ of both photon angles in the far-field (the x-axis is defined as the axis connecting the centers of the two far-field spots). Indeed, in both cases the simulation predicts that our schemes produce the desired N00N states. The simulated coincidence signals show peaks only when both photons are detected at the same far-field angle, while having the same angular spread as that of the far-field intensity spots in Figs. 2(a)-(b). Figure 2(d) also shows a faint circle, which is due to correlations between non-collinear parasitic signal and idler photons which are emitted on two different paths rather than in one. The wavevector scheme is shown in the inset of Fig. 2(d). This effect does not occur for the shaped-pump scheme.

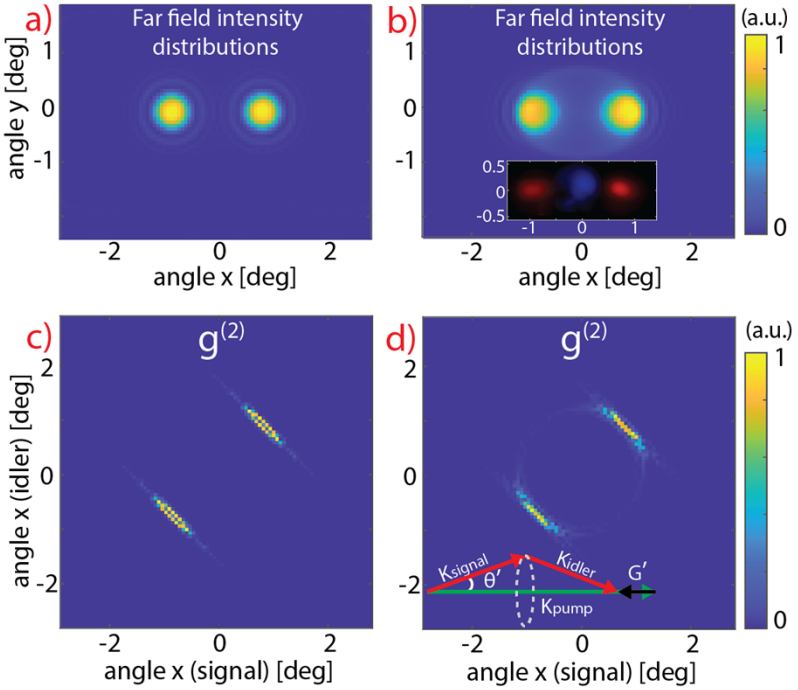

Fig. 2. Simulated far-field intensity distributions of the SPDC signal for the shaped pump (a) and V-patterned crystal (b) schemes, demonstrating emission into two distinct modes in the far-field. Simulated two-photon correlations, $g^{(2)}$, along the x-axis angle (the axis connecting the two far-field modes) for the shaped pump beam (c) and shaped crystal (d) schemes, respectively. The simulations predict the expected bunching of the two photons in either of the two modes, and nearly no additional emission to other directions. The inset in (b) is a raster scan image qualitatively showing the output far field from the V-shaped crystal. Pump residual field is artificially colored in blue and the SPDC emission in red. The inset in (d) shows the wavevector scheme for the process responsible for the faint ring (see text).

Optics EXPRESS

The coincidence measurement results for the pump shaping configuration are presented in Fig. 3(a) for 0.6mW, 6mW and 60mW nominal pump powers (measured after the 532nm line filter) with a 1nm bandpass filter at 1064nm. The dots are the measured coincidence counts and the solid line is their fit to a squared cosine function. As can be seen in the figure, the linear ratio between the pump power and maximum rate of coincidence counts is maintained, in accordance with the linear response of the SPDC process. As shown in Fig. 3(a), we measured a coincidence rate of >200kHz which, normalized to the power, gives 4.2 kHz/mW. This rate constitutes a 1-5 orders of magnitude higher detection rate with respect to previous reported coincidence rates of path entangled N00N states [13,14,16,28,29,33]. These results were achieved with a count rate of $\sim 1.6 \times 10^6$ Hz on one detector and $\sim 2.7 \times 10^6$ Hz on the second detector, hence the average collection efficiency is 12.5%. As expected, the interference patterns show maxima when the phase difference between the arms is a multiple of π instead of multiple of 2π as in classical interference. It can also be observed how the visibility slightly deteriorates by increasing the power: The values we measured are 0.88, 0.81, 0.79 for 0.6, 6 and 60 mW pump power, respectively. We note that the fringe visibility is directly related to the degree of entanglement of the two-photon state [38,39].

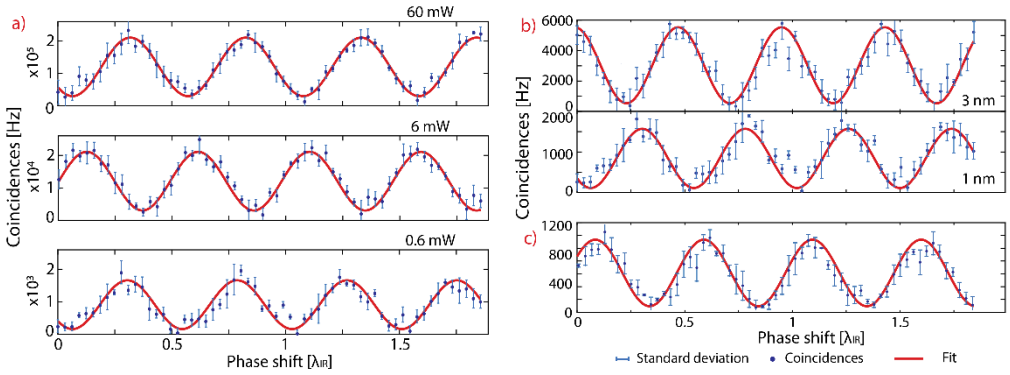

Fig. 3. (a) Coincidence measurements for the pump shaping setup. Measurements were acquired at different pump powers, 60 mW (top), 6 mW (middle) and 0.6 mW (bottom), with an interference filter of 1 nm. (b) Comparison between filtering the down converted photons by 3nm and 1nm band pass filters (top and bottom plots respectively) for 0.6mW pump power. (c) Interference results when the phase shift precedes the NLC on one of the pump arms, for 0.6mW pump power and 1nm bandpass filter. In all the plots, blue dots are the experimental mean values, and the error bars represent the standard deviation of the measured data. The red lines correspond to fits with a squared cosine function.

Figure 3(b) shows a comparison between filtering the down-converted photons by 1 nm and 3 nm band pass filters for 0.6 mW pump power. The comparison was done at a low pump power because when we attempted to use the full pump power of 60 mW with the 3 nm filter, the count rate was so high that it saturated the detectors. As can be seen, the use of the wider interference filter increases the number of coincidences but also slightly decreases the fringe visibility, from ~0.86 to ~0.82. The change in visibility with the different filters should not be attributed to their bandwidth since the two-photons coherence length [33] is much longer than the coherence length defined by the filter bandwidth. The non-perfect visibility at all cases is mainly due to imperfect coupling to the fibers, that includes more than one spatial mode. Photons from different modes can be therefore detected, leading to parasitic coincidences.

It is interesting to note that for the pump shaping configuration, the glass plate could also induce the phase shift by placing it before the NLC, in one of the pump arms. The phase shift in the plate is $\Delta\emptyset = \Delta L(\theta) \cdot 2\pi n/\lambda$ (n is refractive index, $\Delta L(\theta)$ is the angle-dependent optical path

Optics EXPRESS

in the plate, and λ is the wavelength) hence the phase shift of the pump is twice the phase shift of the down-converted photons. Consequently, when the plate is located in the path of the pump beam the phase shift is twice relative to the case where the plate is located on the path of the SPDC photons. However, in a phase-matched degenerate down-conversion process, assuming the un-depleted pump approximation, the phase relation is: $\varphi_{pump} + 2\varphi_{SPDC} = Const$ [40]. Hence, shifting the phase of the single photon 532nm beam before the NLC, is equivalent to shifting the biphotons 1064nm beam after the NLC. The results of this case are presented in Fig. 3(c) for a 0.6mW pump power and 1nm bandpass filter. As seen in the figure, the oscillating pattern in the coincidence counts also has maxima every π phase shift.

Figures 4 presents the experimental results for the patterned crystal configuration. The interference data for a pump power of 60mW are presented in Figs. 4(a) and 4(b), for the cases of 3nm bandwidth line filter and 1nm line filter, respectively. As expected, the results show a periodic oscillating dependence on the relative phase shift, and the period of the coincidence is twice faster with respect to the expected period of classical light interference. Note that for the V-shaped crystal, the maximum number of coincidences with 60mW pump power is of the same order of magnitude as fothe pump shape configuration. However, in the latter case, with a much lower pump power of 0.6mW. This is probably due to the non-collinear phase matching scheme that decreases the overlap between the pump and signal modes, and hence decreases the efficiency and may even impair the mode-matching to the SM fiber. In addition, the V-shaped crystal is 1.5 times shorter and its facets did not have anti-reflection coating. These effects can explain the lower efficiency. The fringe visibility of the 3nm data is about 0.67 while that of the 1nm data is about 0.71.

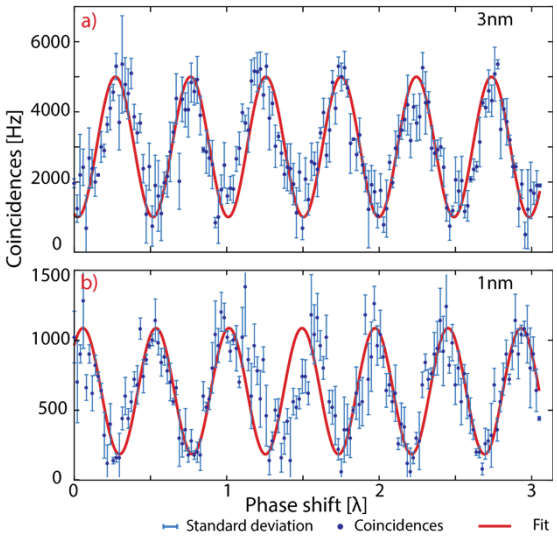

Fig. 4. (a) Coincidence rate for the V-shaped patterned crystal setup. The emission is filtered by a 3nm band pass filter and, in (b) by 1nm band pass filter. In both plots, blue dots and error bars are the experimental mean values and standard deviations respectively, and the red line is a fit to a squared cosine function.

To conclude, two schemes to directly generate path entangled N00N states were presented. Both setups enable to control the spatial properties of SPDC photons, to simplify the setup by generating the state directly from the crystal and to improve the brightness compared to previous schemes [28,29]. As theoretically expected, both setups show an interference pattern with de Broglie wavelength of $\lambda/2$ which is consistent with super-resolution measurements. Our

Optics EXPRESS

record-high rate of N00N state coincidences suggests that these sources can be useful tools for quantum metrology applications. The direct generation concept we introduced here can be further extended to measure 4-photon N00N states, to generate bright squeezed vacuum [41], to generate multimode N00N state [42] either by shaping the pump or the crystal poling and to control spectral and polarization properties of the down-converted photons.

Funding. Israel Academy of Sciences and Humanities; Ministry of Science, Technology and Innovation; Israel Science Foundation (1415/17, 2085/18).

Acknowledgments. The authors acknowledge support from Tel Aviv University Center for Quantum Science and Technology.

Disclosures. The authors declare no conflicts of interest

Data availability. Data underlying the results presented in this paper are not publicly available at this time but may be obtained from the authors upon reasonable request.

References

1. R. Horodecki, P. Horodecki, M. Horodecki, and K. Horodecki, "Quantum entanglement," Rev. Mod. Phys. **81**(2), 865–942 (2009).
2. N. Brunner, D. Cavalcanti, S. Pironio, V. Scarani, and S. Wehner, "Bell Nonlocality," Rev. Mod. Phys. **86**(2), 419–478 (2014).
3. M. A. Nielsen and I. L. Chuang, "Quantum Computation and Quantum Information" (Cambridge University, 2000).
4. T. D. Ladd, F. Jelezko, R. Laflamme, Y. Nakamura, C. Monroe, and J. L. O'Brien, "Quantum computers," Nature **464**(7285), 45–53 (2010).
5. A. Aspuru-Guzik and P. Walther, "Photonic quantum simulators," Nat. Phys. **8**(4), 285–291 (2012).
6. S. Lloyd, "Universal Quantum Simulators," Science **273**(5278), 1073–1078 (1996).
7. N. Gisin, G. Ribordy, W. Tittel, and H. Zbinden, "Quantum Cryptography," Rev. Mod. Phys. **74**(1), 145–195 (2002).
8. C. L. Degen, F. Reinhard, and P. Cappellaro, "Quantum sensing," Rev. Mod. Phys. **89**(3), 035002 (2017).
9. D. J. Wineland, J. J. Bollinger, W. M. Itano, F. L. Moore, and D. J. Heinzen, "Spin Squeezing and Reduced Quantum Noise in Spectroscopy," Phys. Rev. A **46**(11), R6797–R6800 (1992).
10. S. F. Huelga, C. Macchiavello, T. Pellizzari, A. K. Ekert, M. B. Plenio, and J. I. Cirac, "On the Improvement of Frequency Standards with Quantum Entanglement," Phys. Rev. Lett. **79**(20), 3865–3868 (1997).
11. V. Giovannetti, S. Lloyd, and L. Maccone, "Quantum Metrology," Phys. Rev. Lett. **96**(1), 010401 (2006).
12. N. Friis, D. Orsucci, M. Skotiniotis, P. Sekatski, V. Dunjko, H. J. Briegel, and W. Dür, "Flexible Resources for Quantum Metrology," New J. Phys. **19**(6), 063044 (2017).
13. J. G. Rarity, P. R. Tapster, E. Jakeman, T. Larchuk, R. A. Campos, and M. C. Teich, "Two-photon interference in a Mach-Zehnder interferometer," Phys. Rev. Lett. **65**(11), 1348–1351 (1990).
14. M. W. Mitchell, J. S. Lundeen, and A. M. Steinberg, "Super-resolving phase measurements with a multiphoton entangled state," Nature **429**(6988), 161–164 (2004).
15. T. Nagata, R. Okamoto, J. L. OBrien, K. Sasaki, and S. Takeuchi, "Beating the standard quantum limit with four-entangled photons," Science **316**(5825), 726–729 (2007).
16. I. Afek, O. Ambar, and Y. Silberberg, "High-NOON states by mixing quantum and classical light," Science **328**(5980), 879–881 (2010).
17. S. Slussarenko, M. M. Weston, H. M. Chrzanowski, L. K. Shalm, V. B. Verma, S. W. Nam, and G. J. Pryde, "Unconditional violation of the shot-noise limit in photonic quantum metrology," Nat. Photonics **11**(11), 700–703 (2017).
18. J. P. Dowling, "Quantum optical metrology – the lowdown on high-N00N states," Contemp. Phys. **49**(2), 125–143 (2008).
19. A. N. Boto, P. Kok, D. S. Abrams, S. L. Braunstein, C. P. Williams, and J. P. Dowling, "Quantum interferometric optical lithography: exploiting entanglement to beat the diffraction limit," Phys. Rev. Lett. **85**(13), 2733–2736 (2000).
20. M. D'Angelo, M. V. Chekhova, and Y. Shih, "Two-photon diffraction and quantum lithography," Phys. Rev. Lett. **87**(1), 013602 (2001).
21. Y. Israel, S. Rosen, and Y. Silberberg, "Supersensitive polarization microscopy using noon states of light," Phys. Rev. Lett. **112**(10), 103604 (2014).
22. M. Bergmann and P. van Loock, "Quantum error correction against photon loss using NOON states," Phys. Rev. A **94**(1), 012311 (2016).
23. A. Christ, A. Fedrizzi, H. Hübel, T. Jennewein, and C. Silberhorn, "Parametric down-conversion," In *Experimental Methods in the Physical Sciences* Vol. 45, pp. 351–410. Academic Press (2013).
24. A. V. Burlakov, M. V. Chekhova, O. A. Karabutova, D. N. Klyshko, and S. P. Kulik, "Polarization state of a biphoton: Quantum ternary logic," Phys. Rev. A **60**(6), R4209–R4212 (1999).
25. A. Lohrmann, C. Perumangatt, A. Villar, and A. Ling, "Broadband pumped polarization entangled photon-pair source in a linear beam displacement interferometer," Appl. Phys. Lett. **116**(2), 021101 (2020).

Optics EXPRESS

26. P. G. Evans, R. S. Bennink, W. P. Grice, T. S. Humble, and J. Schaake, "Bright source of spectrally uncorrelated polarization-entangled photons with nearly single-mode emission," Phys. Rev. Lett. **105**(25), 253601 (2010).
27. M. Fiorentino and R. G. Beausoleil, "Compact sources of polarization-entangled photons," Opt. Express **16**(24), 20149–20156 (2008).
28. E. Megidish, A. Halevy, H. S. Eisenberg, A Ganany-Padowicz, N. Habshoosh, and A. Arie, "Compact 2D nonlinear photonic crystal source of beamlike path entangled photons," Opt. Express **21**(6), 6689–6696 (2013).
29. H. Jin, P. Xu, X. W. Luo, H. Y. Leng, Y. X. Gong, W. J. Yu, and S. N. Zhu, "Compact engineering of path-entangled sources from a monolithic quadratic nonlinear photonic crystal," Phys. Rev. Lett. **111**(2), 023603 (2013).
30. F. Setzpfandt, A. S. Solntsev, J. Titchener, C. W. Wu, C. Xiong, R. Schiek, T. Pertsch, D. N. Neshev, and A. A. Sukhorukov, "Tunable generation of entangled photons in a nonlinear directional coupler," Laser Photonics Rev. **10**(1), 131–136 (2016).
31. R. Kruse, L. Sansoni, S. Brauner, R. Ricken, C. S. Hamilton, I. Jex, and C. Silberhorn, "Dual-path source engineering in integrated quantum optics," Phys. Rev. A **92**(5), 053841 (2015).
32. A. Arie and N. Voloch, "Periodic, quasi-periodic, and random quadratic nonlinear photonic crystals," Laser Photonics Rev. **4**(3), 355–373 (2010).
33. K. Edamatsu, R. Shimizu, and T. Itoh, "Measurement of the Photonic de Broglie Wavelength of Entangled Photon Pairs Generated by Spontaneous Parametric Down-Conversion," Phys. Rev. Lett. **89**(21), 213601 (2002).
34. A. Gatti, E. Brambilla, K. Gallo, and O. Jedrkiewicz, "Golden ratio entanglement in hexagonally poled nonlinear crystals," Phys. Rev. A **98**(5), 053827 (2018).
35. E. Lantz, N. Treps, C. Fabre, and E. Brambilla, "Spatial distribution of quantum fluctuations in spontaneous down-conversion in realistic situations," Eur. Phys. J. D **29**(3), 437–444 (2004).
36. S. Trajtenberg-Mills, A. Karnieli, N. Voloch-Bloch, E. Megidish, H. S. Eisenberg, and A. Arie, "Simulating Correlations of Structured Spontaneously Down-Converted Photon Pairs," Laser Photonics Rev. **14**(3), 1900321 (2020).
37. E. Rozenberg, A. Karnieli, O. Yesharim, S. Trajtenberg-Mills, D. Freedman, A. M. Bronstein, and A. Arie, "Inverse design of quantum holograms in three-dimensional nonlinear photonic crystals," In *2021 Conference on Lasers and Electro-Optics (CLEO)*, (2021).
38. A. Abouraddy, B. Saleh, A. Sergienko, and M. Teich, "Degree of entanglement for two qubits," Phys. Rev. A **64**(5), 050101 (2001).
39. G. Jaeger, A. Shimony, and L. Vaidman, "Two interferometric complementarities," Phys. Rev. A **51**(1), 54–67 (1995).
40. R. Baumgartner and R. L. Byer, "Optical parametric amplification," IEEE J. Quantum Electron. **15**(6), 432–444 (1979).
41. M. V. Chekhova, G. Leuchs, and M. Żukowski, "Bright squeezed vacuum: Entanglement of macroscopic light beams," Opt. Commun. **337**, 27–43 (2015).
42. S. Hong, J. Rehman, Y. S. Kim, Y. W. Cho, S. W. Lee, H. Jung, S. Moon, S. W. Han, and H. T. Lim, "Quantum enhanced multiple-phase estimation with multi-mode N00N states," Nat. Commun. **12**(1), 1–8 (2021).